



UNIVERSITY OF LEEDS

This is a repository copy of *Sub-marine palaeoenvironments during Emeishan flood basalt volcanism, SW China: implications for plume-lithosphere interaction during the Capitanian ('end Guadalupian') extinction event.*

White Rose Research Online URL for this paper:
<http://eprints.whiterose.ac.uk/87198/>

Version: Accepted Version

Article:

Jerram, DA, Widdowson, M, Wignall, PB et al. (4 more authors) (2016) Sub-marine palaeoenvironments during Emeishan flood basalt volcanism, SW China: implications for plume-lithosphere interaction during the Capitanian ('end Guadalupian') extinction event. *Palaeogeography, Palaeoclimatology, Palaeoecology*, 441 (1). 65 - 73. ISSN 0031-0182

<https://doi.org/10.1016/j.palaeo.2015.06.009>

© 2015, Elsevier. Licensed under the Creative Commons Attribution-NonCommercial-NoDerivatives 4.0 International
<http://creativecommons.org/licenses/by-nc-nd/4.0/>

Reuse

Unless indicated otherwise, fulltext items are protected by copyright with all rights reserved. The copyright exception in section 29 of the Copyright, Designs and Patents Act 1988 allows the making of a single copy solely for the purpose of non-commercial research or private study within the limits of fair dealing. The publisher or other rights-holder may allow further reproduction and re-use of this version - refer to the White Rose Research Online record for this item. Where records identify the publisher as the copyright holder, users can verify any specific terms of use on the publisher's website.

Takedown

If you consider content in White Rose Research Online to be in breach of UK law, please notify us by emailing eprints@whiterose.ac.uk including the URL of the record and the reason for the withdrawal request.



eprints@whiterose.ac.uk
<https://eprints.whiterose.ac.uk/>

1 **Sub-marine palaeoenvironments during Emeishan flood basalt volcanism,**
2 **SW China: implications for plume-lithosphere interaction during the**
3 **Capitanian ('end Guadalupian') extinction event.**

4 **Dougal A. Jerram^{1,2}, Mike Widdowson³, Paul B. Wignall⁴, Yadong Sun^{4,5}, Xulong Lai⁵, David**
5 **P.G. Bond⁴, and Trond H. Torsvik^{1,6,7}.**

6 ¹ Centre for Earth Evolution and Dynamics (CEED), University of Oslo, Norway. (email
7 Dougal@dougalearth.com).

8 ² DougalEARTH Ltd., Solihull, UK (www.dougalearth.com)

9 ³ Department of Earth Sciences, Open University, Walton Hall, Milton Keynes MK7 6AA, UK

10 ⁴ School of Earth and Environment, University of Leeds, Leeds LS2 9JT, UK

11 ⁵ Key Laboratory of Geobiology and Environmental Geology, China University of Geosciences,
12 Wuhan 430074, P. R. China

13 ⁶NGU Geodynamics, Trondheim, Norway

14 ⁷School of Geosciences, University of Witwatersrand, South Africa

15

16 **Abstract**

17 Plume-induced lithospheric uplift and erosion are widely regarded as key features of large igneous
18 province (LIP) emplacement, as is the coincidence of LIP eruption with major extinction and oceanic
19 anoxic events (OAE). The Emeishan LIP, which erupted during the Capitanian (formally 'end
20 Guadalupian') extinction event, has provided the most celebrated example where advocates argue that
21 in excess of 500 m of axisymmetric uplift occurred over >30 000 km² causing extensive radially-
22 distributed erosion and alluvial fan formation. However, the recognition of submarine and

23 phreatomagmatic-style volcanism, as well as syn-volcanic marine sediments interbedded in the
24 eruptive succession, now requires further examination to this simple plume – uplift model. Here we
25 present data from newly-discovered sections from the center of the putative uplifted area (around
26 Lake Er Hai, SW Yunnan Province,) that provide a more complete history of the Emeishan
27 volcanism. These reveal that platform carbonate deposition was terminated by rapid subsidence,
28 followed quickly by the onset of volcanism. For at least the lower two thirds of the 4-5 km thick lava
29 pile, eruptions continued at or below sea level, as testified by the presence of voluminous mafic
30 volcanoclastic deposits, pillow lavas and development of syn-volcanic reefal limestones in the
31 Emeishan inner zone. Only in the later stages of eruption did terrestrial lava flows become widely
32 developed. This onset of volcanism in a submarine setting and the consequent violent,
33 phreatomagmatic-style eruptions may have exacerbated the cooling effects of volcanism during the
34 Capitanian. The late Permian of SW China at the time of the Emeishan was an extended area of
35 thinned lithosphere with epeiric seas, which appear to have been sustained through the onset of LIP
36 emplacement. Therefore, whilst there remains substantial geochemical support of a plume origin for
37 Emeishan volcanism, LIP emplacement cannot be ubiquitously associated with regional pre-eruption
38 uplift particularly where complex lithospheric structure exists above a plume.

39

40 **Introduction and rationale**

41 Large igneous provinces (LIPs) in the form of continental flood basalts, represent the largest lavas
42 outpourings recorded on the planet (Bryan and Ernst, 2008), and are commonly linked with the ascent
43 of mantle plumes (e.g. Richards et al., 1989) from the lowermost mantle (Burke et al. 2008, Torsvik et
44 al. 2008), and with mass extinction events (Wignall, 2001; Courtillot & Renne 2003). Plume-
45 generated continental uplift is predicted to precede LIP volcanism (Campbell and Griffiths, 1990; He
46 et al., 2003; Saunders et al., 2007) although evidence for this phenomenon is difficult to obtain either
47 because it is buried beneath the lava piles themselves, or because preferential weathering and erosion
48 of ancient examples removes less resistant clastic materials which might otherwise provide evidence

49 for pre-eruptive uplift and erosion (White and Lovell, 1997; Jerram and Widdowson, 2005). However,
50 the Middle Permian Emeishan LIP of SW China preserves the basal contact of the volcanics in many
51 locations, and interpretation of these have provided the quintessential, but highly debated, example of
52 axisymmetric pre-eruption mantle plume doming (He et al. 2003, 2006, 2010; Saunders et al. 2007;
53 Ali et al. 2010). The province is also linked to mass extinction late in the Guadalupian (e.g. Zhou et
54 al., 2002) with the extinctions in South China shown to precisely coincide with the eruption onset
55 (Wignall et al. 2009) and carbon isotope perturbations (Bond et al., 2010). Any major uplift events
56 and the resultant volcanic styles will clearly help our understanding of the environmental impact of
57 the province, and its role in the extinction.

58 Initial uplift estimates indicated > 1 km of elevation over an area greater than 400 km radius
59 (He et al. 2006) although the uplift figure has recently been reduced to < 500 m (He et al. 2010).
60 Recent investigation of the basal part of the lava pile reveals that Emeishan volcanism was initially
61 characterised by a phreatomagmatic phase indicating eruptions at, or below, sea level and not, as
62 argued by He et al. (2010), upon uplands elevated to c.500 m (Ukstins Peate & Bryan 2008; Wignall
63 et al. 2009a; Sun et al. 2010). However, because these phreatomagmatic deposits were described from
64 sections around the periphery of the 'inner zone' of uplift as envisaged by He et al. (2006, 2010), the
65 possibility of pre-eruption uplift remains (Ali et al. 2010).

66 Pangea formed in the Late Carboniferous (about 320 million years ago) but South China only
67 became part of the supercontinent in the Late Triassic (see Fig. 1a). In the Late Permian, South China
68 was a separate continent with passive margins toward North China and Annamia (Indochina) and an
69 active eastern margin facing the Panthalassa Ocean. Palaeomagnetic data position South China
70 confidently on equatorial latitudes in the Late Permian (Fig. 1b). The Emeishan LIP (ELIP) erupted
71 from in equatorial latitudes, with contemporaneous tropical humid conditions evinced by widespread
72 coal-measures (Wang et al. 2011; Boucot et al. 2013) and shallow marine carbonates. Coal-bearing
73 and carbonate successions are very common, and the coal-forming materials are interpreted to be
74 derived from marine mangrove-like plants (e.g. Shao et al. 1998). Ancient longitude cannot be
75 determined from palaeomagnetic data, but South China is located in longitude (Torsvik et al. 2008,

76 2014) in such a way that ELIP was sourced by a deep plume from the eastern margin (red line in Fig.
77 1b; the so-called plume generation zone) of the Pacific Large Low Shear-wave Velocity Province in
78 the lowermost mantle (Burke et al., 2008). The Permian of SW China was an extended area of pre-
79 thinned lithosphere partially inundated by epeiric seas; this structurally complex, attenuated
80 lithosphere would have promoted surfaceward advection and emplacement of magma from the plume
81 feeding the ELIP (e.g., Sobolev et al., 2011).

82 Here we present new data from sections within this “inner zone” of the ELIP that reveal accelerated
83 subsidence immediately prior to, and during, the eruption of the main volcanic succession. These
84 indicate that crustal response to plume impingement during ELIP emplacement was complex,
85 producing a collage of uplifted blocks and basinal areas, with extensive marine environments existing
86 well within the volcanic succession. These conditions were more analogous to the volcano-tectonic
87 development of the Palaeogene North Atlantic margin, which developed mixed subaerial and
88 submarine environments (e.g. Jerram et al., 2009; Jones et al., 2012), than an homogeneous regional
89 doming resulting from a simple LIP-uplift evolutionary model.

90

91 **History of emplacement of the Emeishan LIP**

92 The ELIP erupted c. 260 Myrs ago (Zi et al., 2010), and is temporally linked with a Capitanian
93 (Middle Permian) extinction event (Wignall et al 2009; Bond et al. 2010). The “inner zone” is centred
94 on the north-western Panzhihua City, Sichuan Province (Fig. 2). The newly-discovered outcrops
95 studied here occur on the eastern border of Lake Er Hai, approximately 100 km to the south-west of
96 Dali city. Regional dip is to the north, and the contact between the volcanics and underlying Maokou
97 Formation limestones is seen at Wa Se village in the southern-most section, and is repeated by
98 faulting at Shuang Lang town. Due to faulting, the total thickness of the lava pile is difficult to
99 estimate accurately, but it is likely to be 4-5 kilometres, making it one of the thickest known
100 successions (Ali et al. 2005), and is consistent with its location within the central portion of the main
101 Emeishan outcrops. This area has been placed at the centre of the Province (e.g. He et al. 2006, 2010),

102 however the extensive faulting and possible missing/eroded portions of the ELIP make this somewhat
103 difficult to exactly constrain. A generalized section up through the sequence is presented in figure 3
104 along with some key geological features, which are elaborated on below.

105

106 Upper Maokou Formation

107 Shuang Lang (25° 54.612'N 100° 11.679'E). A thick section (>100m) of bioclastic packstones with a
108 diverse fauna including fusulinaceans (*Neoschwagerina*) is cross-cut by several dykes (e.g. figure 3f)
109 (the largest being 15 m in width) that have well developed baked zones (c. 5 m thick) of coarsely re-
110 crystallised limestones. The thickness of both dykes and aureoles indicates these to have been major,
111 and long-lived magmatic feeders, and provide clear evidence that the overlying volcanic succession is,
112 in part, locally sourced. Normally the volcanic sources (volcanoes/fissures etc.) for the ELIP are not
113 well known but with the dykes discovered here it helps highlight that the Lake Er Hai region was near
114 to lava feeder centres within the Emeishan Province.

115 Maokou Fm/Emeishan volcanic succession contact

116 Wa Se (25° 49.2912'N 100° 13.773'E). Thick section of Maokou Formation with foraminifera-peloid
117 packstones capped by a karstic surface displaying kamnitzas (dissolution hollows) with 30 cm of
118 relief. This surface is overlain by 10-40 cm of dark radiolarian-spiculitic wackestones indicative of
119 deeper water conditions than seen in the underlying Maokou Formation (Sun et al. 2010). The ensuing
120 beds consist of ~20 m of red clays with devitrified angular volcanic clasts and a succession of
121 alternating ~10m thick pillow basalt layers separated by further red clays (Figure 3e). The clays are
122 likely derived from submarine plumes or clouds of hyaloclastite. The location of these pillows and of
123 other sections containing pillows throughout the Emeishan (see figure 1), indicate that a substantial
124 area was under water at the onset of the volcanism. This sedimentary – volcanic contact can be traced
125 along strike for several hundred meters up a hillside and does not display any evidence of a 10 – 200
126 m-scale karstic topography invoked in domal uplift models (He et al. 2003, 2010; Ali et al. 2010).

127 Mid Emeishan succession

128 Haichaohe (25° 56.265'N 100° 10.524'E). Quarry showing 20 m thick succession of breccia
129 composed of Maokou limestone clasts, occasionally showing weak alignment, set in a matrix of
130 siliceous, spiculitic mudstone and interbedded with thin beds of lapilli tuff. Clasts show intense
131 recrystallization and are < 1 m in size, except for a large block of limestone in the centre of the quarry
132 section which is 10 m thick and >30 m wide (figure 3b). Conodont samples from this block yielded
133 late forms of *Jinogondolella errata* indicating a basal Capitanian early J. *postserrata* zonal age
134 (Wardlaw and Nestell, 2010).

135 Jiang Wei South (25° 56.607'N 100° 10.096'E). A 55 m thick road cut section showing, in ascending
136 order, coarse basaltic agglomerate, meter-bedded coarse lapilli tuffs, silt grade tuffs and basaltic
137 conglomerate containing sub-rounded to sub-angular clasts set in a fine grained glassy (now de-
138 vitrified) hyaloclastic matrix (e.g. figure 3c-d). The attributes of the last bed suggest some
139 sedimentary reworking but in the lower beds clasts are angular, some with 'jig-saw fit' textures
140 revealing in-situ fracturing and/or cooling and lack of subsequent transport. These are interpreted to
141 be mafic volcanoclastic deposits; a common feature in the Emeishan succession (Ukstins Peate and
142 Bryan 2008). Within the volcanoclastic successions, marine fauna are found (e.g. figure 4), which
143 provide unequivocal evidence for eruption in a marine setting with the central part of the Emeishan
144 province.

145 Upper Emeishan succession

146 Jiang Wei (25° 57.818'N 100° 08.518'E). Basaltic lava flows dominate exposures around Jiang Wei
147 town; these are subaerial sheet flows with well-preserved flow fronts and inflated cores (e.g. figure
148 3a). Several isolated outcrops of limestone c. 50m thick are embedded in this basaltic landscape: one
149 quarry face example reveals a massive Tubiphytes-calcisponge reef, the top surface of which shows a
150 highly irregular topography that records either the original reef surface or localised karstification.
151 Impressively, the overlying lava flow infills this topography and irregular masses of lava occur as
152 "cave fills" up to 8 m below the top contact (figure 5).

153

154

155 **Discussion**

156 Our field observations demonstrate that the exposed stratigraphy in the central part of the Emeishan is
157 clearly predominantly of marine origin. This marine palaeoenvironment clearly existed well beyond
158 the onset of flood volcanism in the region, and highlights a complex story of the evolution of the ELIP
159 with implication for both uplift and for the associated biological crisis discussed below.

160 **(i) Implications for uplift**

161 The Lake Erhai sections reveal that much of the volcanic activity near the centre of the province
162 began in submarine environments, and followed a deepening event in the latest phase of the Maokou
163 Formation. The volcanic facies distributed along the Lake Erhai section are depicted in figure 6. In
164 this regard, the region is geologically similar to those developed toward the periphery where platform
165 collapse and deepening is also observed to have preceded eruption (e.g. Wignall et al. 2009; Sun et al.
166 2010). It also supports the recent observations of thick hydrovolcanic units within other newly
167 reported ‘inner zone’ sections, in the Dali area (Zhu et al., 2014). The transition from pillow basalt
168 volcanism through to predominantly hyaloclastites (described as palagonite-rimmed lapilli-tuffs by
169 Zhu et al. 2014) in the mid-Emeishan succession could represent shallowing of the marine
170 environment, possibly with volcanoclastic rocks prograding into the marine environment (e.g. Jerram
171 et al 2009). Indeed the infilling of existing accommodation space within the marine
172 palaeoenvironment of the ‘inner zone’ by the flood basalts would see a swallowing upwards in the
173 cycle (Zhu et al., 2014). Prevalence of diverse pyroclastic activity in all but the latest stages of the
174 eruption history, reveals continuation of shallow marine emplacement and associated
175 phreatomagmatic style eruptions (Ukstins Peate & Bryan, 2008; Zhu et al., 2014). Only in the later
176 stages of the LIP eruptions do sub-aerial flood basalt flows become developed, and even in this part of
177 the lava stratigraphy interbedded Tubiphytes reefs demonstrate a close balance between emplacement
178 and subsidence that kept the growing volcanic edifice at, or close to, sea-level. Such microbial reefs

179 are common within the Emeishan lava pile and indicative of a post-extinction carbonate facies
180 analogous to the widespread stromatolite reefs which follow the end-Permian extinction (Pruss et al.
181 2005). Since this base level did not change significantly during emplacement of a several kilometres
182 thick volcanic pile rapid subsidence must have kept pace with aggradation throughout most of the
183 brief eruption history (~1 myr, Ali et al. 2005, Wignall et al. 2009).

184 The current work, makes clear that the pattern of uplift and subsidence is complex within both the
185 peripheral and central regions of the Emeishan LIP, and is in agreement with Sun et al. (2010).
186 Maokou limestone deposition spanned the Roadian-Capitanian stages, and the dating of the
187 Haichaohe block shows it was sourced from the younger part of the Formation. Accordingly, erosion
188 of Maokou limestone must have begun after onset of Emeishan eruptions, with clasts incorporated
189 into a depositional systems where both sediment-gravity flows and giant glide blocks (e.g. at
190 Haichaohe) were depositing. The entrainment of small, angular fragments of mafic and carbonate
191 material in these strata indicates either minimal sediment transport distances, or else that they were
192 sourced during brecciation of the Maokou Formation by explosive volcanism.

193 It has been proposed previously either that 100s m of the Maokou Formation were removed, either
194 down to lowermost Roadian levels, or the Formation was removed entirely in this “inner zone” (e.g.
195 He et al. 2003, 2010). However, discovery of large blocks from the upper Maokou Formation
196 (Capitanian Stage) embedded within the middle of the Emeishan volcanics indicates that this is not
197 the case. Similarly, the lack of erosion at the basal contact argues against pre-volcanic uplift, and that
198 depositional base level only approached sea level late in the eruptive history as revealed by
199 calcimicrobial reefs preserved between upper lava successions. One possible explanation for the
200 records of a spectacular, high relief, prevolcanic karst landscape may in fact derive from locations in
201 the upper part of the Emeishan volcanics where isolated outcrops of intra-trappean limestone
202 (typically reefs) embedded in flood basalts could simulate an apparent mega-karst landscape. Previous
203 arguments for uplift have hinged on the interpretation of volcanoclastic beds as alluvial deposits (He et
204 al., 2003) and have already been countered with the suggestion that they represent primary
205 hydromagmatic volcanism (Ukstins Peate & Bryan, 2008; Wignall et al. 2009).

206 Mantle plume updoming models predict that locations in the centre of the province, such as those
207 studied here, should have experienced deep erosion. However, a simple plume head model is
208 inadequate at explaining all of the observed sedimentary and palaeontological evidence. LIPs can
209 often contain volcanoclastic deposits at the onset of flood volcanism dependent on the
210 palaeoenvironments at eruption (e.g. Ross et al; 2003), their existence and importance is often
211 underestimated due to poor exposure or overlooked. It is known from examples elsewhere, (e.g. North
212 Atlantic Igneous Province; Wrangellia, Canada), that rapid, transient elevation changes result in
213 complex patterns of erosion and sedimentation both prior to, and during flood volcanism, (e.g.,
214 Saunders et al., 2007; Greene et al., 2008; Jones et al., 2010). This is especially the case in regions of
215 heterogeneous lithosphere because plume – lithosphere interactions are conditioned not only by the
216 dynamics of the rising plume head (Sleep 1997), but also by the interaction of the plume with
217 rheology and structure of the overlying lithosphere, and the far-field stresses affecting that lithosphere
218 (e.g. Burov and Guillou-Frotier, 2005). In effect, plume—generated surface uplift can become
219 significantly modified resulting in affected regions experiencing crustal dilation and/or contraction
220 (Burov and Gerya, 2014). In such cases, pulses of uplift and subsidence of several hundred metres can
221 produce a series of narrow basins (Burov et al., 2007, 2014), with this system of highs and lows
222 evolving into an intra-basin topography with 10s – 100s km wavelengths and attendant patterns of
223 erosion and deposition. The complex tectonic environment at the time of the Emeishan flood basalts,
224 seems to have resulted in a complex surface response to mantle plume impact, and a significant
225 amount of the volcanic material erupted into the sea. This pattern of lithospheric response in ELIP is
226 consistent with that predicted in recent models (Burov et al., 2014), and thus provides an important
227 link between predictive theory and observation.

228 **(ii) Possible effects of sub-marine eruption on end-Guadalupian environment**

229 The onset of volcanism in a submarine setting and the consequent violent phreatomagmatic-style
230 eruptions forming volcanoclastics (Fig. 6) may have exacerbated the cooling effects of volcanism due
231 to the input of volatiles into the stratosphere. Additionally, the input of volcanic material directly into
232 the marine environment would have had significantly different consequences than subaerial eruptions

233 alone. The Capitanian extinction losses are noteworthy for the effect they have on warm-water,
234 photosynthetic groups such as fusulinids foraminifers, calcareous algae and alatoconchid bivalves
235 (e.g. Isozaki & Aljinovic 2009; Wignall et al. 2009) which supports a cooling-driven crisis, although
236 recent studies in the Arctic have discovered an equally severe marine extinction in Boreal latitudes
237 (Bond et al. 2015), coincident with an elevation of mercury concentrations implying an elevation of
238 global volcanism (Grasby et al. in press). The effects of warming, anoxia and acidification may
239 therefore be more applicable to the Capitanian crisis (Bond et al. 2015) suggesting greenhouse gas
240 emissions are also likely to have been substantial. Suggestions that thermogenic carbon dioxide
241 release also amplified the volcanogenic greenhouse gas releases of the Emeishan Province (Ganino &
242 Arndt 2009) is supported by our observations of major feeder dykes with thick contact metamorphic
243 aureoles. However, evaluating the different temperature trends during the Capitanian crisis/Emeishan
244 volcanism awaits a detailed study.

245 **Conclusions**

246 The model for the evolution of the Emeishan in the Lake Erhai section, based on detailed observations
247 of the lithologies and their key relationships is as follows (see figure 4):

- 248 1) The Maokou limestones record a persistent period of shallow-water platform carbonate
249 deposition terminated by a brief emergence (eustatic regression?) and subsequent rapid
250 deepening.
- 251 2) The onset of flood volcanism occurred during this rapid deepening phase and the extrusion of
252 thick sequences of pillow basalts and associated marine sediments. Rapid subsidence
253 persisted until late into the eruption history of the province because only high in the
254 succession are subaerial lavas encountered.
- 255 3) Volcanism continued with the eruption of hyaloclastites in shallow marine environments. The
256 presence of large glide blocks and much smaller clasts of Maokou carbonates indicates either
257 local uplift and erosion of the uppermost parts of this Formation or spectacularly violent
258 eruptions capable of moving blocks tens of meters in dimensions.

- 259 4) The final stages of volcanism are characterised by emergence of the province and
260 development of subaerial lava flows and shallow-water Tubiphytes reefs. This emergence
261 probably resulted from the continuous build-up of the lava pile.
- 262 5) Contrary to most model predictions, the record of uplift, rifting and sedimentation in the ELIP
263 does not conform to the accepted simple, axisymmetric model; this suggests that, each LIP
264 may reveal its own pattern of lithospheric response as a response to regional lithospheric
265 structure and attendant far-field stresses.
- 266 6) Models looking at the causes of the Capitanian extinction event, need to take into account that
267 unlike many predominantly subaerial flood basalt provinces, a significant component of the
268 Emeishan erupted into marine conditions.
- 269 7) Clearly, the volcano-tectonic evolution of the Emeishan LIP is complex, and better
270 understood as a plume-lithosphere interaction that was controlled not only by the thermal
271 dynamic of the plume head, but also by the heterogeneous nature of the Late Permian
272 extended lithosphere of the South China (Fig 1).

273

274 Acknowledgements

275 This work was inspired by discussions with Jason Ali over several years, and funded by NERC grant
276 NE/D011558/1 to PW, Chinese grants: Natural Science Foundation of China (grants nos. 40872002,
277 40921062) and Chinese State Administration of Foreign Experts Affairs (Grant B08030). This work
278 was also partly supported by the Research Council of Norway through its Centres of Excellence
279 funding scheme, project number 223272 (CEED) and the European Research Council under the
280 European Union's Seventh Framework Programme (FP7/2007-2013)/ERC Advanced Grant
281 Agreement Number 267631 (Beyond Plate Tectonics). We would like to thank Eric Font for editorial
282 assistance and Andrea Marzoli and Andy Saunders for constructive reviews.

283

284 References

285 Ali, J. R., Thompson, G. M., Zhou M., Song X., 2005. Emeishan large igneous province, SW China.
286 Lithos 79, 475-489.

287 Ali, J.R., Fitton, J.G., Herzberg, C., 2010. Emeishan large igneous province (SW China) and the
288 mantle-plume up-doming hypothesis. *J. Geol. Soc. Lond.* 167, 953-959.

289 Bond, D.P.G., Hilton, J., Wignall, P.B., Ali, J.R., Stevens, L.G., Sun, Y-D., Lai X-L., 2010. The
290 Middle Permian (Capitanian) mass extinction on land and in the oceans. *Earth-Sci. Rev.* 109,
291 100-116.

292 Bond, D. P. G.; Wignall, P. B., Joachimski, M.M., Sun, Y.-D., Savov, I., Grasby, S.E., Beauchamp,
293 B., Blomeier, D.P.G., 2015. An abrupt extinction in the Middle Permian (Capitanian) of the
294 Boreal Realm (Spitsbergen) and its link to anoxia and acidification. *Bull. Geol. Soc. Amer.* doi:
295 10.1130/B31216.1

296 Bond, D. P. G.; Wignall, P. B. Wang, W. Izon, G. Jiang, H.-S. Lai, X.-L. Sun, Y.-D. Newton, R. J.
297 Shao, L.-Y. Védrine, S., Cope, H., 2010. The mid-Capitanian (Middle Permian) mass extinction
298 and carbon isotope record of South China. *Palaeogeogr., Palaeoclimatol., Palaeoecol.*, 292, 282–
299 294.

300 Boucot, A.J., Xu, C., Scotese, R., 2013. Phanerozoic paleoclimate: An atlas of lithologic indicators of
301 climate. *SEMP Concepts in Sedimentology and Paleontology* No. 11, Tulsa, Oklahoma, 478 pp.

302 Bryan, S.E., Ernst, R.E., 2008, Revised definition of large igneous provinces (LIPs): *Earth- Sci. Rev.*
303 v. 86, p. 175–202.

304 Burke, K., Steinberger, B., Torsvik, T. H., Smethurst, M. A., 2008. Plume generation zones at the
305 margins of large low shear velocity provinces on the core–mantle boundary. *Earth Planet. Sci.*
306 *Lett.* 265, 49–60.

307 Burov, E., Guillou-Frottier, L., 2005. The plume head-continental lithosphere interaction using a
308 tectonically realistic formulation for the lithosphere. *Geophys. J. Int.* 161, 469-490.

309 Burov, E., Guillou-Frottier, L., d’Acremont, E., Le Pourhiet, L., Cloetingh, S., 2007. Plume head-
310 continental lithosphere interactions near continental plate boundaries. *Tectonophysics* 434, 15-
311 38.

312 Burov, E., Gurya, T., 2014. Asymmetric three-dimensional topography over mantle plumes. *Nature*
313 513, 85-89.

314 Cocks, L.R.M., Torsvik, T.H., 2013. The dynamic evolution of the Palaeozoic geography of eastern
315 Asia. *Earth-Sci. Rev.* 117, 40-79.

316 Courtillot, V.E., Renne, P.R., 2003. On the ages of flood basalt events: *Comp. Rend. Geosci.* 335,
317 113–140.

318 Domeier, M., Torsvik, T.H., 2014. Plate kinematics of the Late Paleozoic. *Geosci. Frontiers* 5, 303-
319 350.

320 Ganino, C., Arndt, N.T. 2009. Climate change caused by degassing of sediments during emplacement
321 of large igneous provinces. *Geology* 37, 323-326.

322 Grasby, S.E., Beauchamp, B., Bond, D.P.G., Wignall, P.B., Sanei, H., in press. Mercury deposition in
323 association with three Permian extinction events in NW Pangea. *Geol. Mag.*

324 Greene, A.R., Soates, J.S., Weis, D., 2008. Wrangellia flood basalts in Alaska: A record of plume-
325 lithosphere interaction in a Late Triassic oceanic plateau. *Geochem. Geophys. Geosyst.* 9(12).
326 DOI:10.1029/2008GC002092

327 He B., Xu Y., Chung S.L., Xiao L., Wang Y., 2003. Sedimentary evidence for a rapid, kilometer-scale
328 crustal doming prior to the eruption of the Emeishan flood basalts. *Earth Planet. Sci. Lett.* 213,
329 391-405.

330 He B., Xu Y., Wang Y., Luo Z., 2006. Sedimentation and lithofacies paleogeography in SW China
331 before and after the Emeishan flood volcanism: New insights into surface response to mantle
332 plume activity. *J. Geol.* 114, 117-132.

333 He B., Xu Y., Campbell, I., 2009. Pre-eruptive uplift in the Emeishan? *Nature Geoscience* 2, 530-531.

334 He B., Xu Y., Guan J.-P., Tong, Y-T., 2010. Paleokarst on top of the Maokou Formation: further
335 evidence for domal crustal uplift prior to the Emeishan flood volcanism. *Lithos* 119, 1-9

336 Isozaki, Y., Aljinovic, D., 2009. End-Guadalupian extinction of the Permian gigantic bivalve
337 *Alatoconchidae*: end of gigantism in tropical seas by cooling. *Palaeogeogr. Palaeoclimatol.*
338 *Palaeoecol.* 284, 11-21.

339 Jerram, D. A., Widdowson, M., 2005. The anatomy of Continental Flood Basalt Provinces: geological
340 constraints on the processes and products of flood volcanism. *Lithos* 79, 385-405.

341 Jerram, D. A., Single, R.T, Hobbs, R.W., Nelson, C.E., 2009. Understanding the offshore flood basalt
342 sequence using onshore volcanic facies analogues: an example from the Faroe–Shetland basin
343 *Geol. Mag.* 146,. 353–367.

344 Jones, S.M., Lovell, B., Crosby, A.G., 2012. Comparison of modern and geological observations of
345 dynamic support from mantle convection. *J. Geol. Soc. Lond.* 169, 745-758.

346 Pruss, S.B., Corsetti, F.A., Bottjer, D.J., 2005. The unusual sedimentary rock record of the Early
347 Triassic: A case study from the southwestern United States. *Palaeogeogr. Palaeoclimatol.*
348 *Palaeoecol.* 222, 33-52.

349 Richards, M.A., Duncan, R.A., Courtillot, V.E., 1989. Flood Basalts and Hot-Spot Tracks: Plume
350 Heads and Tails. *Science*, 246, 103-107.

351 Ross, P.-S., Ukstins Peate, I., McClintock, M.K., Xu, Y.G., Skilling, I.P., White, J.D.L., Houghton,
352 B.F., 2003. Mafic volcanoclastic deposits in flood basalt provinces: a review. *J. Volcan.*
353 *Geotherm. Res.* 145, 281-314.

354 Saunders, A. D., Jones, S. M., Morgan, L. A., Pierce, K. L., Widdowson, M., Xu Y.-G., 2007.
355 Regional uplift associated with continental large igneous provinces: The roles of mantle plumes
356 and the lithosphere. *Chem. Geol.* 241, 282–318, doi:10.1016/j.chemgeo.2007.01.017

357 Shao, L., Zhang, P., Ren, D., Lei, J., 1998. Late Permian coal-bearing carbonate successions in
358 southern China: coal accumulation on carbonate platforms. *Intern. J. Coal Geol.* 37, 235-256.

359 Sleep, N.H., 1997. Lateral flow and ponding of starting plume material. *J. Geophys. Res.* 102, 10001-
360 10012.

361 Sobolev, S.V., Sobolev, A.V., Kuzmin, D.V., Krivolutskaya, N.A., Petrunin, A.G., Arndt, N.T.,
362 Radko, V.A., Vasiliev, Y.R., 2011. Linking mantle plumes, large igneous provinces and
363 environmental catastrophes. *Nature* 477, 312-316.

364 Sun Y-D., Lai X-L., Wignall, P.B., Widdowson, M., Ali, J.R., Jiang H-S., Wang W., Yan C-B., Bond,
365 D.P.G., Védrine, S., 2010. Dating the onset and nature of the Middle Permian Emeishan large

366 igneous province eruptions in SW China using conodont biostratigraphy and its bearing on
367 mantle plume uplift models: *Lithos*, 119, 20-33.

368 Torsvik, T.H., Steinberger, B., Cocks, L.R.M. Burke, K., 2008. Longitude: Linking Earth's ancient
369 surface to its deep interior. *Earth Planet. Sci. Lett.* 276, 273-283.

370 Torsvik, T.H. Burke, K., Steinberger, B., Webb, S.C. Ashwal, L.D., 2010. Diamonds sourced by
371 plumes from the core mantle boundary. *Nature* 466, 352-355

372 Torsvik, T.H., Van der Voo, R., Doubrovine, P.V., Burke, K., Steinberger, B., Ashwal, L.D., Trønnes,
373 R., Webb, S.J., Bull, A.L., 2014. Deep mantle structure as a reference frame for movements in
374 and on the Earth. *Proc. Nat. Acad. Sci.* 111, 24, 8735–8740.

375 Wang, H., Shao, L., Hao, L., Zhang, P., Glasspool, I.J., Wheelley, J.R., Wignall, P.B., Yi, T., Zhang,
376 M., Hilton, J., 2011. Sedimentology and sequence stratigraphy of the Lopingian (Late Permian)
377 coal measures in southwestern China. *Int. J. Coal Geol.* 85, 168-183.

378 Wardlaw, B.R., Nestell, M.K., 2010. Three *Jinogondolella* apparatuses from a single bed of the Bell
379 Canyon Formation in the Apache Mountains, West Texas: *Micropaleo.* 56, 195-212.

380 White, N. & Lovell, J.P.B., 1997. Measuring the pulse of a plume with the sedimentary record. *Nature*
381 387, 888-891.

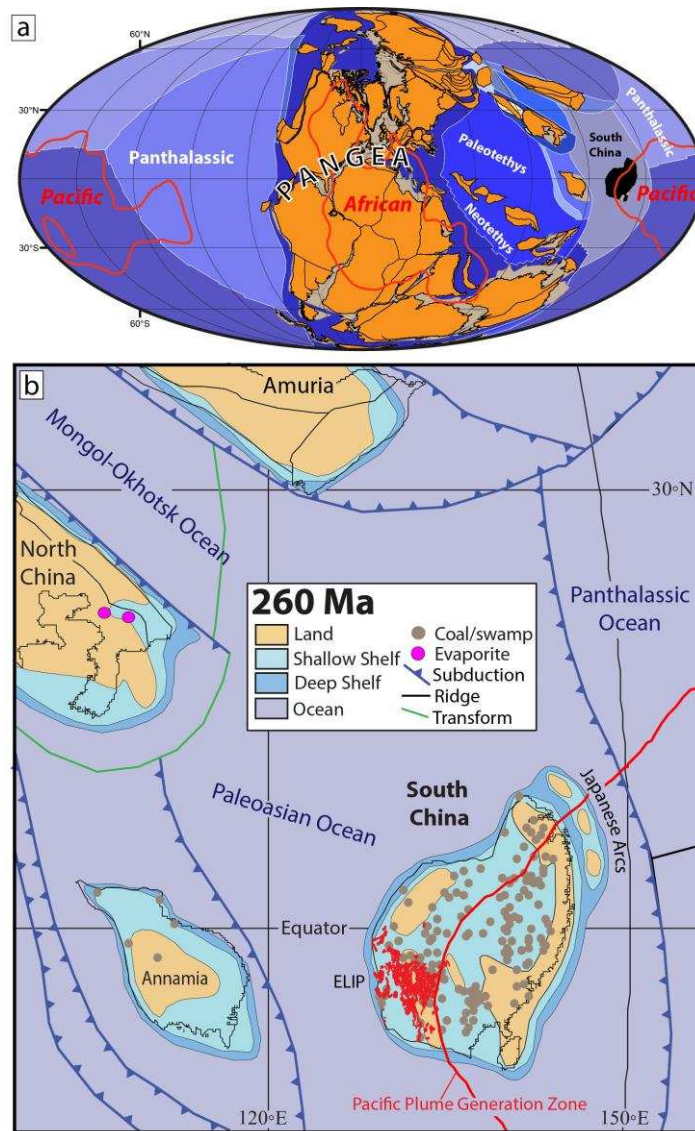
382 Wignall, P.B., 2001. Large igneous provinces and mass extinctions. *Earth-Sci. Rev.* 53, 1–33.

383 Wignall, P.B., Sun Y-D., Bond, D.P.G., Izon, G., Newton, R.J., Védrine, S., Widdowson, M., Ali,
384 J.R., Lai X-L., Jiang H-S., Cope, H, Bottrell, S.H., 2009. Volcanism, mass extinction and
385 carbon isotope fluctuations in the Middle Permian of China. *Science* 324, 1179-1182.

386 Zhou M-F., Malpas, J., Song, X-Y., Robinson, P.T., Sun, M., Kennedy, A.K. Leshner, C.M., Keays,
387 R.R., 2002. A temporal link between the Emeishan large igneous province (SW China) and the
388 end-Guadalupian mass extinction. *Earth Planet. Sci. Lett.* 196, 113-122.

389 Zhu, B. Guo, Z., Liu, R., Liu, D., Du, W., 2014. No pre-eruptive uplift in the Emeishan large igneous
390 province: New evidences from its ‘inner zone’, Dali area, Southwest China. *J. Volcanol.*
391 *Geotherm. Res.* 269, 57–67.

392 Zi J.-W., Fan, W.-M., Wang, Y.-J., Cawood, P.A., Peng, T.-P. Sun, L.-H., Xu, Z.-Q., 2010. U-Pb
393 geochronology and geochemistry of the Dashibao Basalts in the Songpan-Ganzi Terrane, SW
394 China, with implications for the age of Emeishan volcanism. *Amer. J. Sci.* 310, 1054-1080.
395
396
397
398
399
400

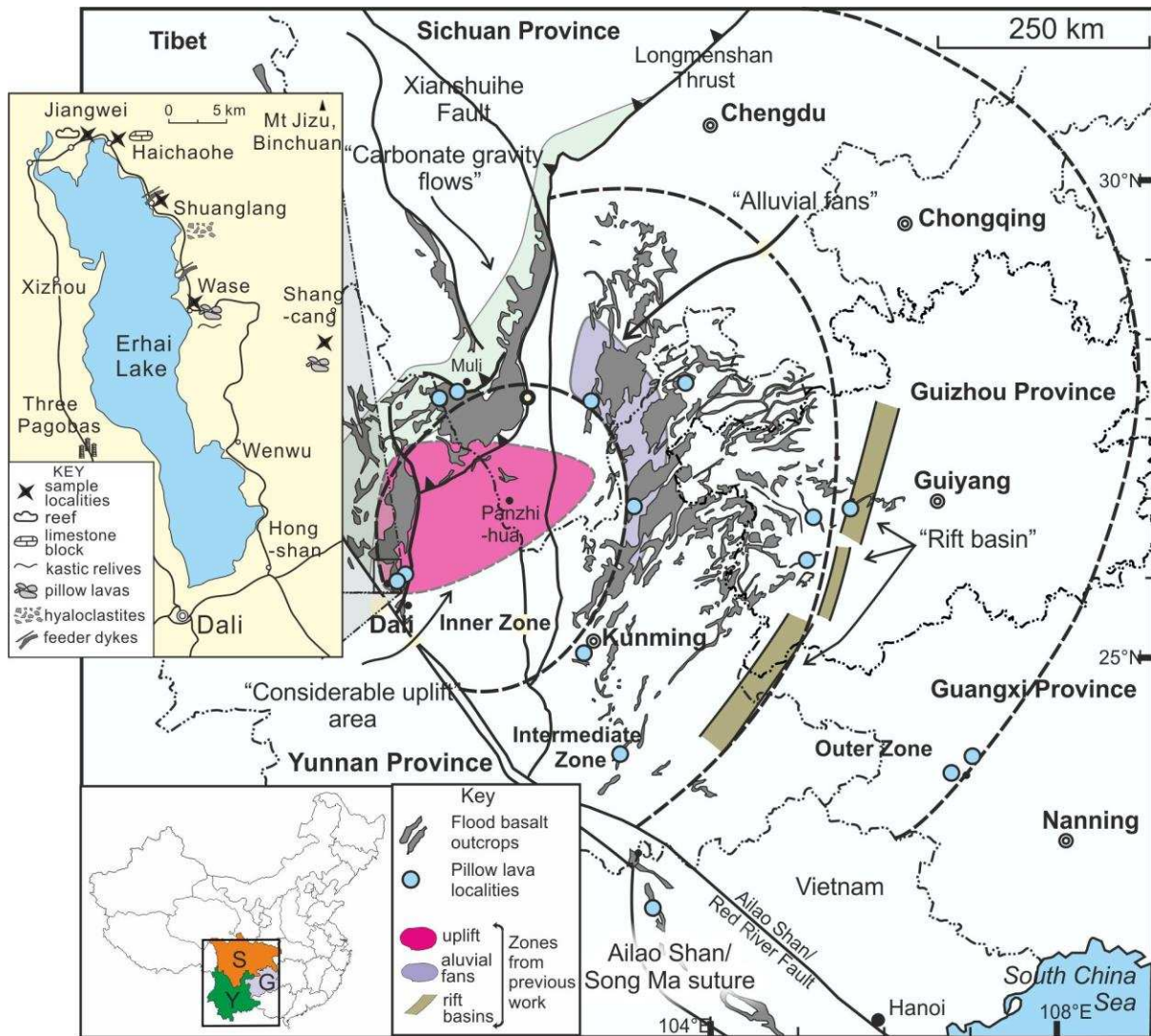


401

402 Figure 1. (a) Global palaeomagnetic plate reconstruction (Molweide projection) at 260 Ma (Domeier & Torsvik
 403 2014). Pangea formed in the Late Carboniferous but early breakup is witnessed already in the Early
 404 Permian by opening of the Neotethys. Cimmerian terranes leaving Pangea included parts of Iran,
 405 Turkey, Afghanistan, Tibet, Burma, Thailand and Malaysia (Sibumasu). Since Pangea formed, plumes
 406 that sourced the majority of Large Igneous Provinces and kimberlites have been derived from the
 407 edges of two stable and antipodal thermochemical reservoirs at the core-mantle boundary beneath
 408 Africa and the Pacific (Torsvik et al. 2008, 2010, 2014; Burke et al. 2008). South China cannot be
 409 related to Pangea by plate circuits but using (assuming) this remarkable surface to deep Earth
 410 correlation we can position South China in longitude in a such a way that ELIP erupted directly above
 411 the Pacific plume generation zone (thick red line). Latitude is derived from palaeomagnetic data and
 412 net true polar wander at 260 Ma is zero (Torsvik et al. 2014).

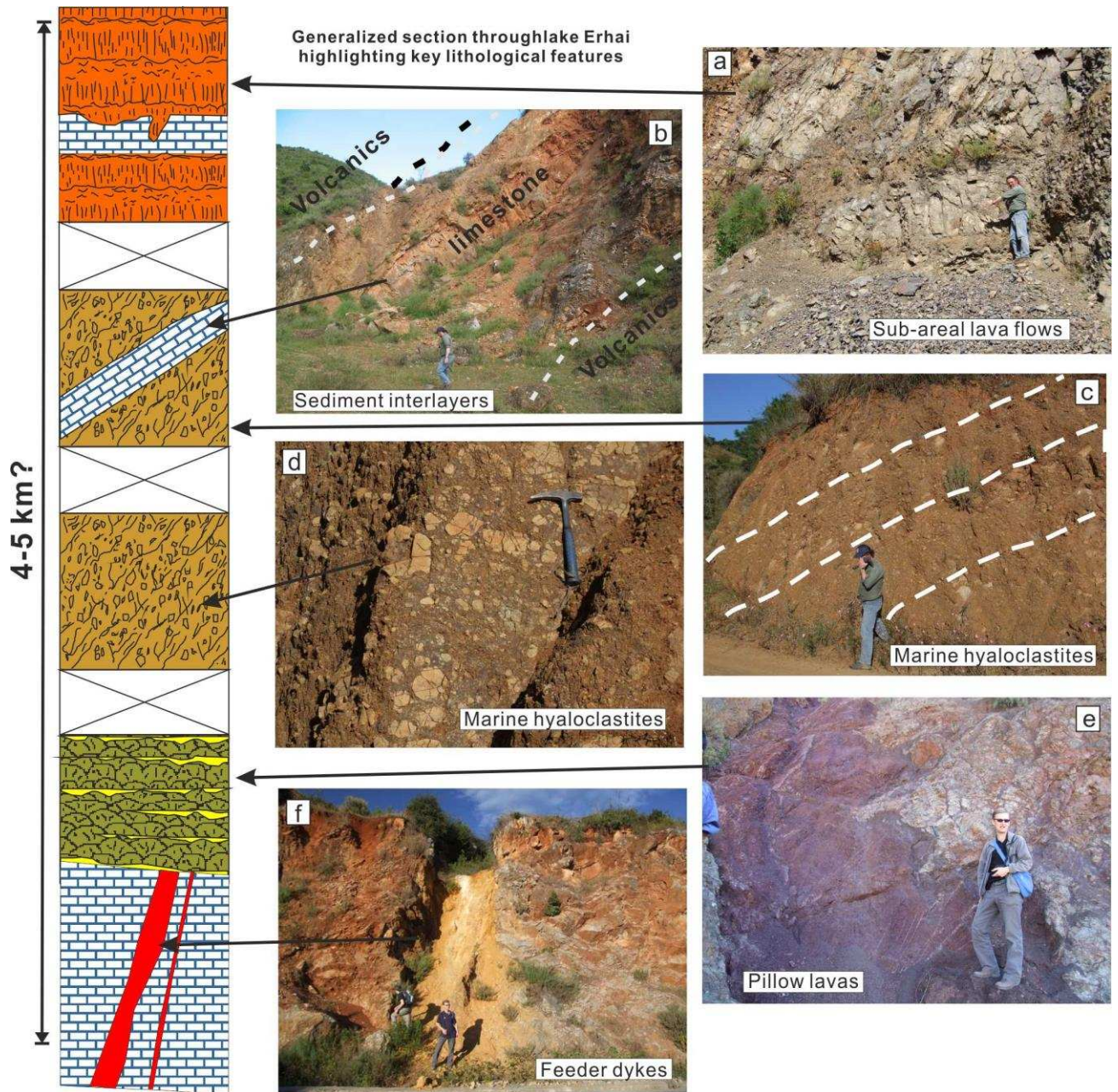
413 (b) Detailed 260 Ma reconstruction of South China, Annamia (Indo-China), North China (including Sulinheev)
 414 and Amuria (Central Mongolia, Hutag Uul-Songliao, Hinggan-Nuhetdavaa and Khanka-Jiamusu
 415 Bureya). The reconstruction with detailed plate boundaries follows Domeier & Torsvik (2014) and
 416 draped with Guadalupian (272-260 Ma) and Lopingian (260-252 Ma) coal/swamp and evaporate
 417 occurrences (Boucot et al. 2013). Indicated areas of Late Permian land, shallow and deep shelf
 418 modified from Cocks & Torsvik (2013) but both facies patterns and plate boundary configurations are
 419 rather dynamic in the Late Permian.

420



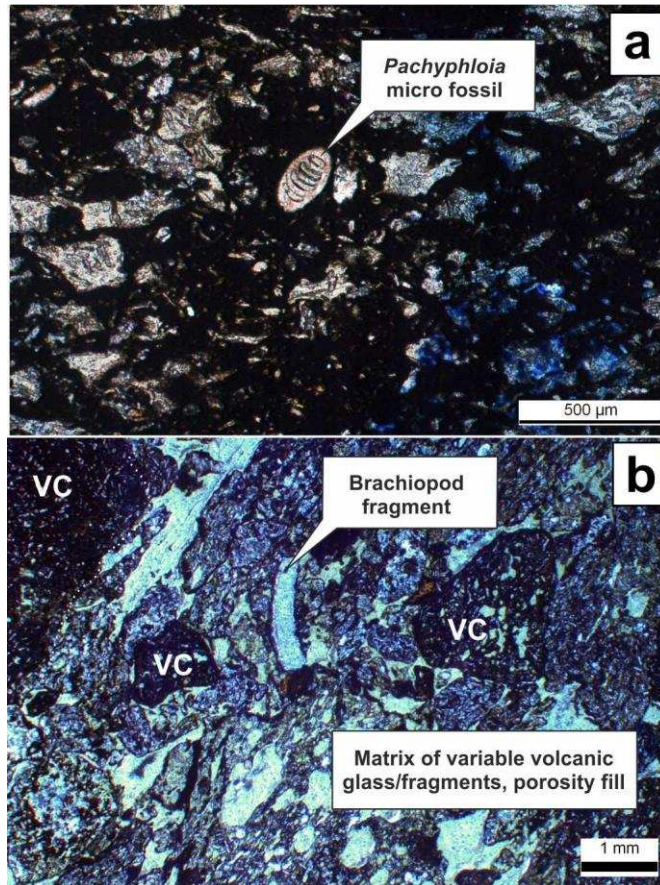
421
 422
 423
 424
 425
 426
 427
 428

Figure 2. Distribution of Emeishan volcanic and location map of the study section found within the originally mapped 'inner zone'. On the main map, locations of pillow lavas sections are indicated as well as the original zones labelled from previous studies (adapted from He et al., 2010). Inset map shows Lake Erhai and the locations that make up the section in figure 3.



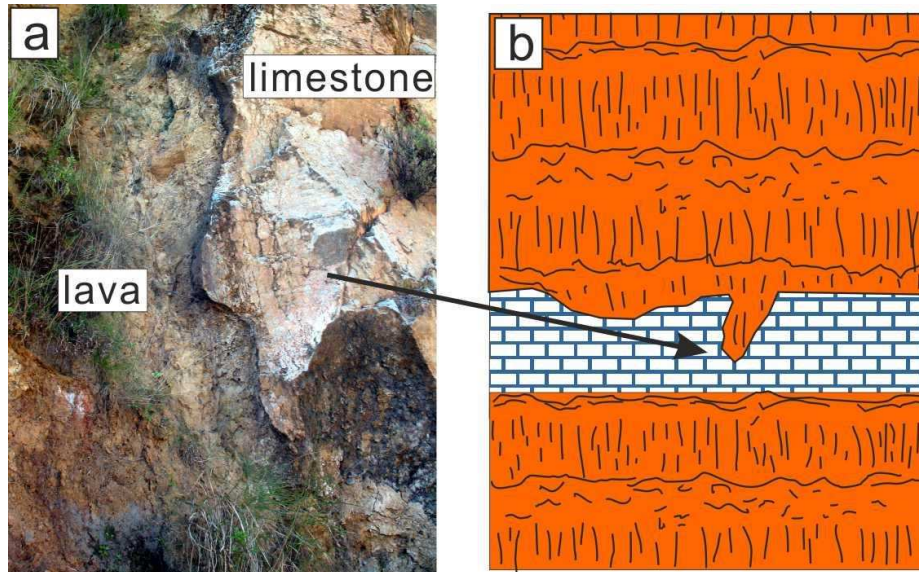
429
 430
 431
 432
 433
 434
 435

Figure 3. Generalised section through the Lake Erhai region. Showing key lithostratigraphic features including: Feeder dykes (f), Pillow lavas (e), Hyaloclastites (d-c), Sediment interlayers (b), and Sub-areal lava flows (a). Overall section covers some 4-5 km.



436
437
438
439
440
441
442

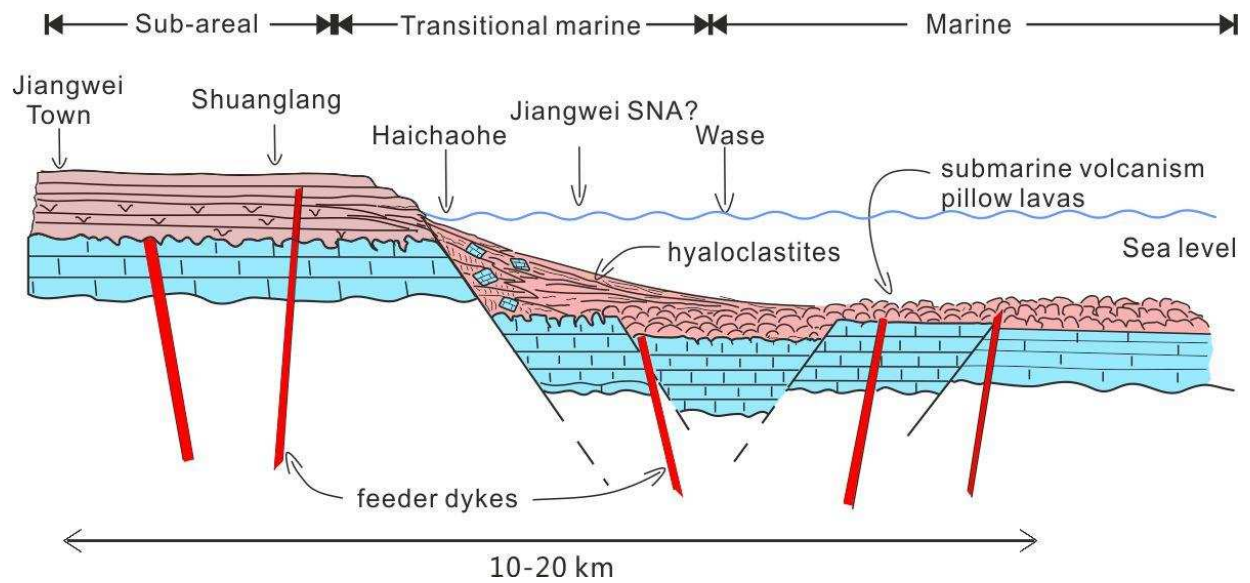
Figure 4. Evidence of marine fauna in volcanoclastics. A) Complete *Pachyphloia* within volcanic glass and fragments. B) Brachiopod shells within volcanic fragments (examples of microcrystalline volcanic clasts marked VC on photomicrograph).



443
444
445
446
447
448

Figure 5. The upper volcanic section highlighting spectacular examples of lava flows into a karst topography within the limestone. This indicates that the upper parts of the volcanic sequence have been erupted into a subareial environment.

Volcanic facies distribution along Lake Erhai section



449
450
451
452
453

Figure 6. Idealized cross section through the volcanic succession along the Lake Erhai section. The onset of flood volcanism in the majority of the section is characterized by submarine volcanism with pillow lavas and hyaloclastites.